Journal of Engineering Physics and Thermophysics, Vol. 82, No. 1, 2009

PARAMETERS OF TIP–SAMPLE INTERACTIONS IN SHEAR MODE USING A QUARTZ TUNING FORK AFM WITH CONTROLLABLE Q-FACTOR

Vo Thanh Tung,[a,b] **S. A. Chizhik,**[a] **and Tran Xuan Hoai**[b]

UDC 539.2:681.2

A quartz tuning fork-based atomic force microscopy for investigating the tip–sample interactions at the nanoscale in the shear-force mode is described. Results of force interactions (damping and elastic forces) can be obtained from the amplitude-phase-distance spectroscopy measurements made with a tuning fork with a tungsten tip and a sample surface. The influence of the interaction between tip and sample using the quality factor as an indicator is investigated. Furthermore, a simple model shows that the extension of a tuning fork-based AFM can be applied to quantitative analysis of the properties of the sample surface.

Keywords: *Tuning fork, shear force, damping force, elastic factor, quality factor.*

Introduction. Since its invention [1], the atomic force microscopy (AFM) has gained remarkable popularity in many fields, e.g., in biological and biophysical researches [2, 3], polymer physics [4, 5], and material sciences [6]. In recent years, scientists have developed the use of AFM for the local measurement of surface properties at the nanoscale resolution. Furthermore, many methods have been developed for using AFM to obtain information on chemical and physical properties of materials at the nanoscale, such as viscoelastic properties, surface potentials, Young modulus, chemical interactions, adhesion, friction, etc. [7–12]. This information is particularly important for understanding the interaction properties of the surface of nanomaterials. In the normal AFM dynamic operation mode, the tip oscillates in the vertical direction (perpendicular to the surface), i.e., in the direction of the forces between atoms in the tip and sample, so that this kind of Van der Waals interaction force plays the dominant role for damping the oscillation. In contrast, in the shear mode the tip oscillates parallel to the surface and we can obtain more information about the surface properties. The damping force is not only the Van der Waals force but includes other interactions such as friction force and absorbent moving interaction.

Quartz tuning forks were originally introduced into the field of scanning probe microscopy (SPM) by Gunther et al. [13] and later by Karrai and Grober [14]. Recently, Giessibl [15] employed them for atomic resolution AFM imaging. Tuning forks were used as sensors at low temperatures and in high magnetic fields by Rychen et al. [16]. The forks have several advantages: high amplitude and phase sensitivities, high mechanical quality factor Q, and large spring constant, which allows the detection of piconewton (pN) forces and the acquisition of true atomic resolution images. The feedback control can be constructed in a fully digital-electronic manner, so that the implementation of the control is greatly simplified. Quartz tuning forks have been successfully used under various conditions [13, 14, 16–18]. However, there are very few studies on the use of quartz tuning fork-based AFM for investigation of surface properties with nanoscale resolution.

Karrai and Tiemann [19] reported the results of the measurements with a tuning fork, which enabled them to detect the friction force in the pN range. In their measurements, the tuning fork was excited by mechanical coupling with an external piezooscillator, so that the Q-factor of the system could not be controlled.

In this paper, we describe the measurement of the shear mode tip–sample interactions of a tuning fork with a tungsten tip on two classes of samples: i) samples with a "nonrigid surface" (soft) (polyethylene and fiber plastic) and ii) a sample with a "rigid surface" (hard) (alumina Al_2O_3) in the shear-force mode operation. In our study, we constructed a controllable Q-factor system, so that we could investigate the tip–sample interaction through variation of the preset qual-

[a]A.V. Luikov Heat and Mass Transfer Institute, National Academy of Sciences of Belarus, P. Brovka Str. 15, Minsk, 220072, Belarus; email: votungbeo@gmail.com; [b]Institute of Applied Physics and Scientific Instrument of the Vietnamese Academy of Science and Technology, Vietnam. Published in Inzhenerno-Fizicheskii Zhurnal, Vol. 82, No. 1, pp. 141–149, January–February, 2009. Original article submitted June 25, 2008.

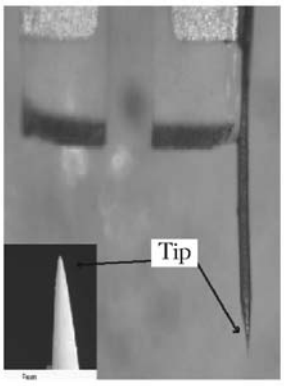

Fig. 1. Scanning electronic microscopy image and optical photograph of tungsten tip attached to quartz tuning fork.

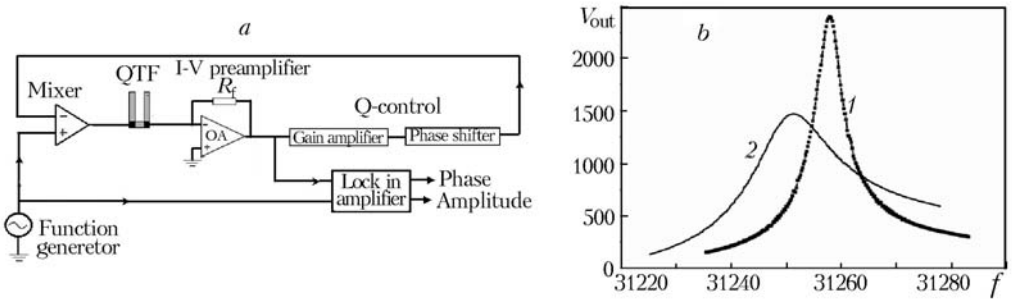

Fig. 2. Block diagram of I-V preamplifier and Q-control system (a) and the resonant frequency curve of tuning fork with tungsten tip (b) without Q-control at Q_∞ = 8119 (1) and with it at Q_∞ = 1833 (2). V_{out}, mV; f, Hz.

ity factor (the meaning of the Q-factor at free oscillation, when the tip is far from the sample surface, is called hereafter Q_∞ for short). The results are interpreted with simple models that consider the damping forces between the tip and the polymer surface and the elastic forces of the polymer around the tip. The influence of the Q-factor on the tip–sample interaction components is investigated. These results show that the capabilities of the combination of a tuning fork-based AFM can be extended to quantitatively analyze the properties of surface of nanomaterials with high precision.

Experimental Setup. Figure 1 shows the force sensor in the experiments. A tuning fork is used as a single quartz cantilever. In the lateral force sensor, the tip is mounted parallel to the tuning fork and oscillates nearly parallel to the surface with fixed amplitude. The quartz tuning forks (QTF) used in the force microscope have a nominal resonant frequency of 32768 Hz, i.e., 2^{15} Hz, a spring constant K = 12 kN calculated from the measured dimensions of the tuning fork, and a quality factor of about 9000 [20]. The tungsten tip fabricated by electrochemical etching with a tip radius of about 50–80 nm is glued to the prong of the tuning fork, as shown in Fig. 1, parallel to one arm of the fork.

This sensor was incorporated into a commercial atomic force microscope, NT-206 (Microtestmachines Co.) [21]. Mechanical and electrical control systems of the AFM NT-206 were used with addition of Q-control capabilities. Q-control allowed us to reduce the Q-factor of the tuning fork. This reduces the settling time to a new resonant frequency and allows the z feedback loop to track the set point more rapidly during operation. As discussed in [22], using the Q-control system, one can obtain better information on small size images than without Q-control and hence improve the imaging resolution. Figure 2a shows the principle of the electrical circuit of Q-control which is connected with the tuning fork gluing the tungsten tip. The motion of the fork is sensed by a current-to-voltage converter which feeds directly into a lock-in amplifier and the Q-control circuit (Fig. 2a). The resulting resonance curves in air before and after using the Q-control system are shown in Fig. 2b.

Dynamic Force Spectroscopy and Theory of Friction and Elastic Forces with Controllable Q-Factor. The amplitude-frequency-distance characteristic was measured during approach only or retraction only to avoid backlash effects. In these measurements, we must set the beginning, the last positions, and the operation step of the probe. At the

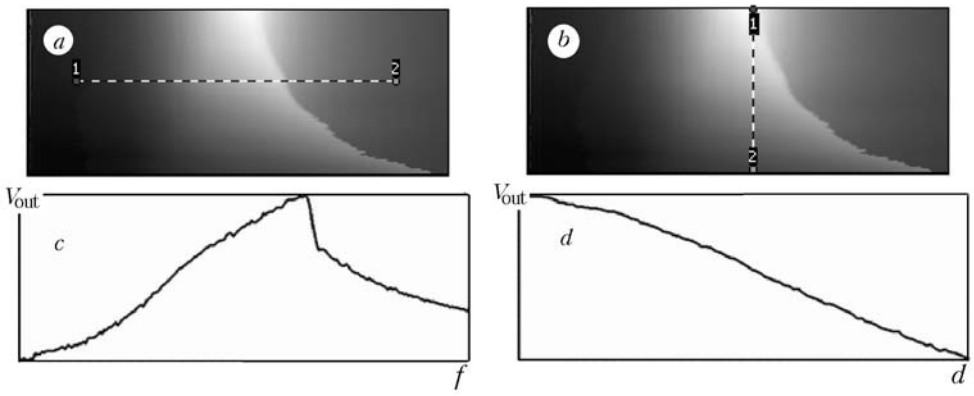

Fig. 3. 2-D images of amplitude-frequency-distance spectroscopy in the dynamic shear-force: amplitude vs. frequency and distance (a and b); the amplitude as a function of frequency (c) at fixed distance along the line 1–2 in Fig. 3a and as a function of distance (d) along the line 1–2 at fixed frequency in Fig. 3b. V_{out}, mV; f, Hz; d, nm.

same time, we also set up the driving frequency, ordinarily around the resonant frequency. When operating, we obtained a frequency dependence of the amplitude, when the tip approaches the surface sample very slowly. Figure 3 shows 2-D images taken in order to investigate the distance dependence of these interactions on polyethylene polymer. In the identical Fig. 3a and b, the tip oscillation amplitude, which is illustrated by light intensity, is shown as a function of frequency (horizontal axis) and the distance between tip and sample (vertical axis).

We analyzed the relationship of amplitude-frequency-distance spectroscopy. The tip position d is determined as the distance from an arbitrary reference point far from the surface, where Q_∞ is preset and d is defined to be zero. Therefore, an increasing d corresponds to decreasing tip/sample separation. At each distance, the amplitude is recorded as a function of frequency. All the data presented are as measured, with no smoothing algorithms applied.

The frequency-dependent oscillation amplitude u of the tuning fork arm using a Q-control system obeys the following Newton equation of motion given by [19, 22]:

$$\frac{\partial^2 u(\tau)}{\partial \tau^2} + \left(\gamma + \gamma_\infty + \frac{g}{\omega}\right)\frac{\partial u(\tau)}{\partial \tau} + \frac{K+k}{M}u(\tau) = \frac{F_d}{M}. \tag{1}$$

The effective mass M of the fork arm, which is proportional to the mass distributed along the tine, is defined as $M = \frac{K+k}{(2\pi f)^2} = 0.966 \cdot 10^{-6}$ kg. The gain g is the adjustable coefficient of Q-control system. The force F_d drives the fork harmonically at the frequency f. The damping of the motion is included in the damping rate term $\gamma + \gamma_\infty$, where subscript ∞ refers to corresponding resonance parameters at the free oscillation. The tip–sample interaction is included in Eq. (1) through the terms k and γ, respectively, where γ is the damping rate intrinsic to the fork, with the tip disengaged from the sample. We can then determine the tip–sample interaction-induced damping rate in relation to γ_∞ as

$$\gamma = \gamma_\infty\left(\frac{f_\infty u_\infty}{fu} - 1\right) + \frac{g}{\omega}\left(\frac{u_\infty}{u} - 1\right), \tag{2}$$

where f_∞ and f are the resonant frequencies of quartz at the free oscillation and at an approached distance for the interaction between tip and sample, respectively.

The damping force $F_f = M\gamma u$, which is due to the tip—sample viscous damping, is a drag force opposing the oscillatory motion of the tip. Using Eqs. (1) and (2), F_f is given by

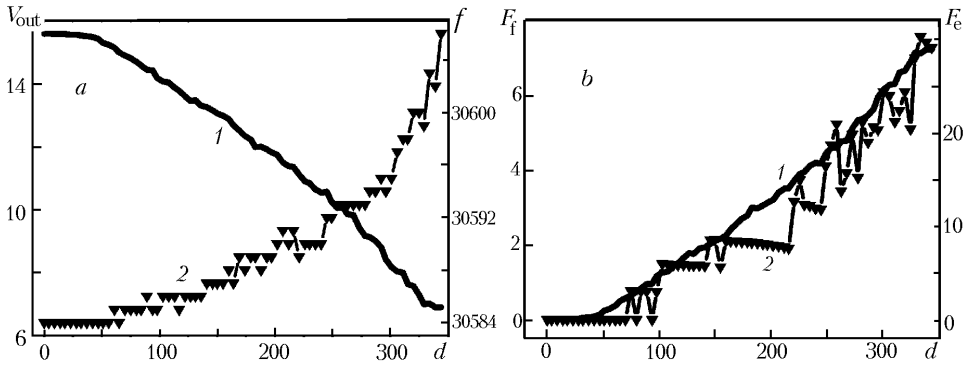

Fig. 4. The tip–sample distance dependences in the case of polyethylene surface: a) amplitude (1) and frequency (2); b) damping force (1) and elastic force (2) interactions. f, Hz; V_{out}, mV; F_f, nN; F_e, nN; d, nm.

$$F_f = \frac{i}{\sqrt{3}} \frac{Ku_\infty}{Q_\infty} \left[\left(1 - \frac{fu}{f_\infty u_\infty} \right) + \left(\frac{Q_\infty}{Q_{eff}} - 1 \right) \left(1 - \frac{u}{u_\infty} \right) \right]. \tag{3}$$

Here, we put the new coefficient Q_{eff}:

$$\frac{1}{Q_{eff}} = \frac{1}{Q_\infty} + \frac{\sqrt{3}\, gM}{K}. \tag{4}$$

The elastic force F_e due to the reactive tip–sample interaction, which is a restoring force along the oscillation motion of the tip, can be expressed as $F_e = ku$. The theoretical spring constant K is obtained as $K = \frac{E}{4} w \left(\frac{t}{l} \right)^3$, where $E = 7.87 \cdot 10^{10}$ N/m^2 is the Young modulus of quartz. With the preset parameters of the tuning fork (width $w \approx 0.38$ mm, thickness $t \approx 0.6$ mm, and length $l \approx 5.00$ mm) we obtain $K = 12$ kN/m, which agrees reasonably well with our experimental result [20]. The local tip—sample interaction equivalent spring constant k can be obtained by using the relation for K in the equation $k = \left[\left(\frac{f}{f_\infty} \right)^2 - 1 \right] K$, which gives F_e as

$$F_e = \left(\frac{f^2}{f_\infty^2} - 1 \right) Ku. \tag{5}$$

To interpret expressions (3) and (5), it is necessary to define the relationship between the measured output voltage V_{out} and the oscillation amplitude of one arm of the tuning fork. The output voltage is sensitive to the antisymmetric mode of the tuning fork; therefore, $V_{out} = c(u_1 - u_2)$, where c is a constant and u_1, u_2 are the amplitudes of motion of two arms of the fork. When driving the fork with an external voltage, as in our experiment, only the antisymmetric mode is excited, yielding $u_1 = -u_2$. Thus, we define: $V_{out} = 2cu_1 = u_1/\alpha$, where $\alpha = 253$ pm/mV (according to [20]).

Using Eqs. (2), (3), (5), and the above relationship between the measured output voltage and the oscillation amplitude of one arm of the tuning fork, we have

$$F_f = \frac{i}{\sqrt{3}} \frac{KV_\infty}{Q_\infty} \alpha \left[\left(1 - \frac{fV_{out}}{f_\infty V_\infty} \right) + \frac{\sqrt{3}\, gM}{K} Q_\infty \left(1 - \frac{V_{out}}{V_\infty} \right) \right], \tag{6}$$

$$F_e = \frac{K}{f_\infty^2} \alpha \left(f^2 - f_\infty^2 \right) V_{out}, \tag{7}$$

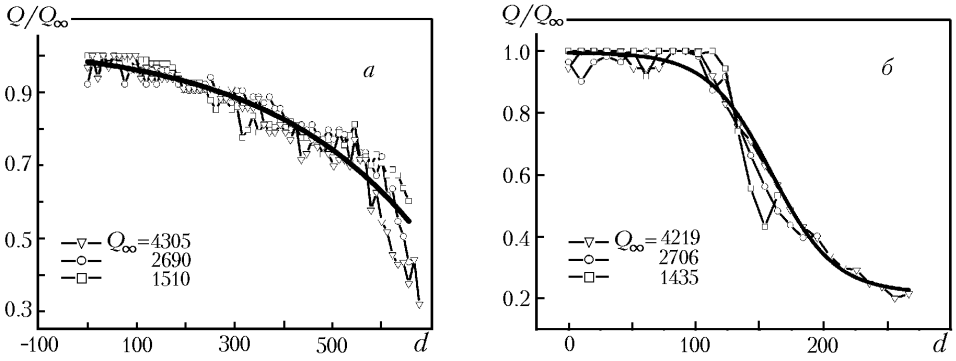

Fig. 5. The tip–sample distance dependence of quality-factor for different preset values of Q_∞ on fiber plastic (a) and alumina (b). The solid curves are the fitting ones of the experimental data. *d*, nm.

where V_∞ is the voltage corresponding to the free vibration of tuning fork. Based on these equations and the experimental data, we measured the amplitude and resonant frequency of the prong of the tuning fork, when approaching the surface of polyethylene, from whence we determined the force of interaction with the sample surface.

Figure 4a shows the dependence between oscillation amplitude and frequency on the distance between tungsten tip and polyethylene surface. Remember, increasing distance *d* decreases tip/sample separation. We used a tuning fork with a tungsten tip at Q_∞ = 1860, resonant frequency of 30,584 Hz, and applied voltage to the fork of 2.32 V. As the tip approaches the surface, the amplitude vs. distance curve shows a monotonic decrease. In contrast, the resonant frequency *f* seems to increase monotonically though it is noisier. It can be seen that the frequency is rather sensitive and, especially closer to the sample surface, this reveals a more pronounced change as compared to the amplitude signal. Therefore, the use of modulated frequency in the near-contact region might give a better signal for distance control.

From the measured values of amplitude and frequency and Eqs. (6), (7), the damping and elastic forces are calculated and shown in Fig. 4b. Initially the damping force does not change until the tip—sample interaction increases and this force begins to change. Similarly to the damping force, the elastic interaction changed negligibly in the preset contact of tip and sample. However, close to the surface, a different form of the elastic force, a "sawtooth" and "unstable" profile, is observed. Therefore we can split the interaction into two regions: 1) the vibrating tip is situated far from the sample, where there is no interaction between the tip and sample, 2) the tip is close to the sample surface (the contact region), here the damping force increases rapidly and monotonically. Our results for the dependence of the amplitude, frequency shift, and force (elastic and damping forces) interactions in Fig. 4a and b are similar to those from [19].

Influence of Preset Quality Factor on the Parameters of Tuning Fork. There have been carried out several experiments by different groups before (see, e.g., [22, 23, 24]), where the influence of Q-control system on spectroscopy curves and on results of scanning has been investigated. However, a quantitative interpretation of those experimental results is still lacking. So, with a clearer understanding, we have surveyed the effect of change of Q_∞ on change of oscillation amplitude and quality factor of the tuning fork. For a better comparison, we specifically chose one tuning fork, using the same applied voltage and measurements under the same conditions of operation, with no change of the area of the sample approached by the tip.

Firstly, we have surveyed the influence of the preset quality factor Q_∞ on the variation of the Q-factor of the tuning fork when the tip approaches the surface of these materials. Figure 5 shows the curves of the quality factor versus the distance on polyethylene and alumina. We see that the quality factor *Q* decreases as the tip–sample distance is reduced. For alumina, the decrease of *Q* is rapid and rather abrupt. For polyethylene, the change in *Q* is slow. However, we do not observe the influence of Q_∞ on these curves. It is seen that the variation of the quality factor *Q* depends only upon the properties of the material surface, not upon Q_∞. Therefore, it would be interesting to use these results for examination of the general structures of the sample surface.

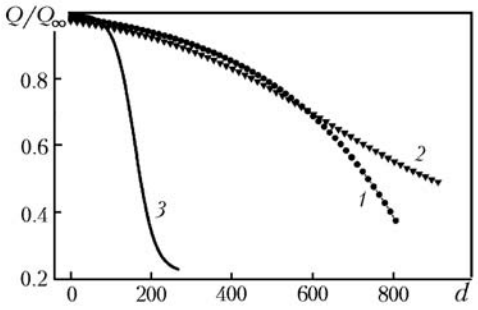

Fig. 6. Fitting of the measured data for dependence of the quality factor on the tip–sample distance for different samples: polyethylene (1), fiber plastic (2), and alumina (3). *d*, nm.

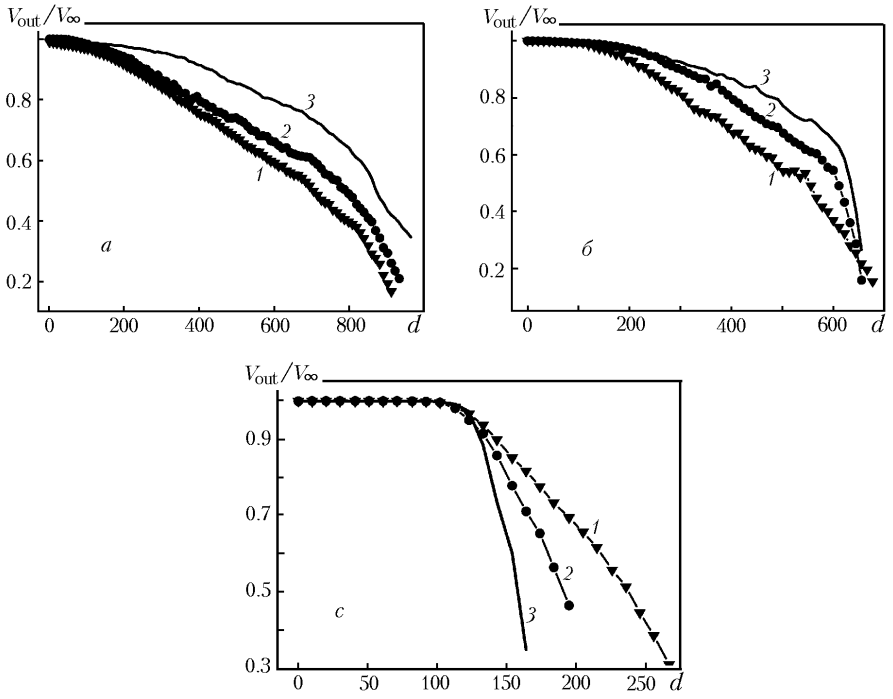

Fig. 7. Dependence of the amplitude on the tip-sample distance for different preset values of the quality factor Q_∞ on polyethylene (a): 1) Q_∞ = 4559, 2) 3039, 3) 1636; fiber plastic (b): 1) Q_∞ = 4305, 2) 2690, 3) 1501; alumina (c): 1) Q_∞ = 4219, 2) 2706, 3) 1435. *d*, nm.

In order to illustrate the application of the variation of the quality factor Q with the kind of sample, we performed the above experiments on three materials: polyethylene, fiber plastic, and alumina Al_2O_3 (see Fig. 6). We observed an obvious difference between these materials. While the change of the slope of Q versus the tip—sample distance for polyethylene and fiber is rather slow, the curve for alumina is much more rapid. Therefore, we are confident that we can expand this measure to identify the surface properties of other "rigid" or "nonrigid" materials.

In order to understand the observed material dependence of the variation of Q with the tip approaching the surface, we make some assumptions for these materials. For the alumina sample, the surface is rather homogeneous and has a rigid structure. In the shear-force mode, the tip oscillates horizontally and abruptly enters into the influence region of the atomic forces. Therefore, the variation of the interaction curves of alumina sample is rather abrupt. In contrast, the surface of polyethylene and fiber plastic has no tight structure and is not smooth. The influence of the atomic forces is not uniform, and the clear bound of the interaction region is absent. So, when approaching closer to

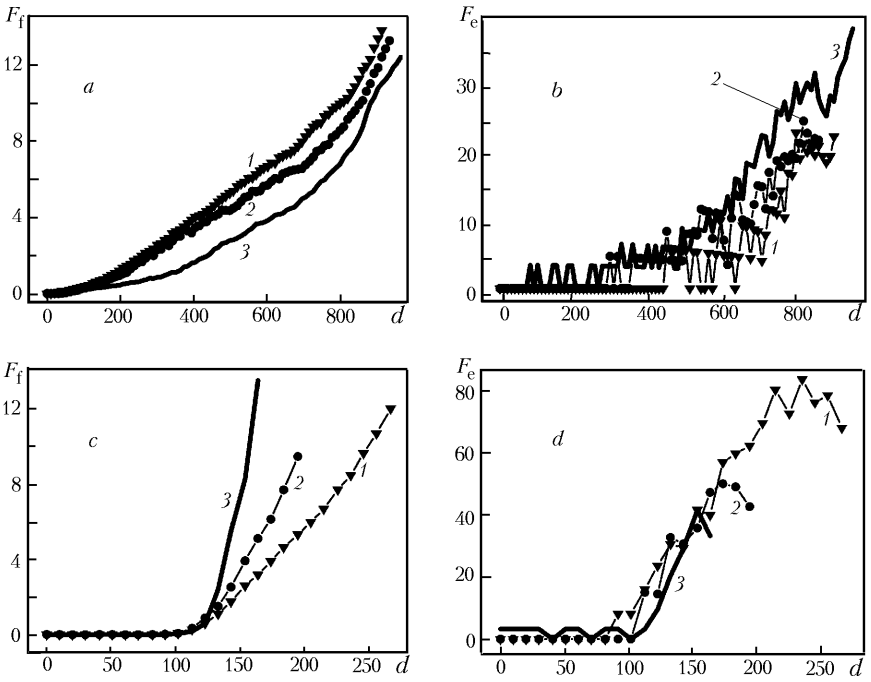

Fig. 8. Dependence of the damping (a and c) and elastic (b and d) forces on the tip–sample distance for different preset values of the quality factor on polyethylene (a and b) and alumina (c and d); the values of Q_∞ in Fig. 8a and b are the same as in Fig. 7a, the values of Q_∞ in Fig. 8c and d are the same as in Fig. 7c. F_f, nN; F_e, nN; d, nm.

the "nonrigid" sample, the tip is affected not suddenly but smoothly. This may be very useful for surveying the properties of surface for different types of samples.

As mentioned above, the variation of the quality factor Q during approach of the tip is not affected by a change of Q_∞. However, the change of the oscillation amplitude is strongly affected by a change of Q_∞. To understand this effect, we measured the change of the oscillation amplitude of the tip as it approached the sample using different preset values of Q_∞ on three samples: polyethylene, fiber plastic, and alumina, as shown in Fig. 7. For alumina, the larger Q_∞, the lower the slope of the curve of the amplitude change versus tip—sample distance. However, the trends for polyethylene and fiber plastic are different. Furthermore, we realize that for "nonrigid" materials at positions closer to the sample, the oscillation amplitude of the tip increases when Q_∞ decreases, which was not observed on alumina. These results show that we can also obtain information on images as well as properties of the surface of "nonrigid" samples more advantageously when Q_∞ decreases. This enabled us to achieve the best scan rate and obtain real time imaging and high resolution with low quality factor Q_∞ [22].

Influence of Preset Quality Factor on the Force Interactions. In Fig. 8 are shown the resulting force interaction curves with different preset values of quality factor on "soft" (polyethylene) and "rigid" (alumina) materials. From these results, we see that for "soft" materials, a clear effect of the influence of the factor Q_∞ on the damping force is observed. At the same distances between the tip and sample, at higher preset factors Q_∞ the damping force is larger (Fig. 8a). These results demonstrate that further reduction of damping force can be achieved by decreasing fork quality factor. We predict that with "soft" materials in these regimes (semi-contact and contact ones), we can change the quality factor and therefore increase the effective tip—sample interaction, which leads to higher stabilization in shear-force operation.

In contrast, for alumina the major difference is observed in the curves for the damping force. It is seen in Fig. 8c that the damping force for alumina depends on Q_∞: the larger Q_∞, the smaller the slope of the damping force curves. It should be noted that we do not compare the increase of the damping force at positions closer to the sample, which correspond to three different preset quality factors Q_∞.

CONCLUSIONS

We have performed dynamic amplitude-frequency-distance spectroscopy measurements and developed a simple model to determine the force interactions (damping and elastic forces) using tuning fork gluing tungsten tips in shear-force mode. A survey of the influence of the preset quality factor (using Q-control) on the interaction components between the tip and sample is presented. The results make it possible to explain the advantages of using a low preset quality factor for tuning forks and to get better information on the surface of "nonrigid" materials. In future, this will provide a simple model to extend applications of the tuning fork based on AFM to qualitative analysis in nanotribology, which will enable one to determine the parameters and properties of the surface of soft materials, such as selection of surface structure of materials, viscosity coefficient, and shear modulus.

The authors would like to thank Professor J. Maps from the University of Minnesota Duluth, USA for helpful discussions.

The work was carried out within the framework of the Belarusian Project 1.9 of SSTP "Scientific Equipment".

NOTATION

c, constant; d, distance from an arbitrary reference point to the surface sample, nm; E, Young modulus of tuning fork, N/m^2; f, resonant frequency of oscillation of tuning fork, Hz; f_∞, resonant frequency of tuning fork at free oscillation, Hz; F_e, elastic force due to reactive tip–sample interaction, nN; F_f, damping force due to tip–sample viscous damping, nN; F_d, driven force for tuning fork, N; g, adjustable coefficient of Q-control system; i, imaginary unity; k, term of excess restoring (the spring constant of the local tip–sample interaction), N/m; K, theoretical spring constant, N/m; l, length of an arm of tuning fork, mm; M, effective mass of an arm of fork, kg; Q, quality factor; Q_{eff}, effective quality factor; Q_∞, quality factor of tuning fork at free oscillation; t, thickness of an arm of fork, mm; u, oscillation amplitude of fork, nm; u_∞, oscillation amplitude of fork at free oscillation, nm; u_1, u_2, amplitudes of motion of two arms of fork, nm; V_{out}, output signal of tuning fork, mV; V_∞, voltage at free vibration of tuning fork, mV; w, width of an arm of tuning fork, mm; α, constant, pm/mV; γ, damping rate term of tip–sample interaction; γ_∞, damping term at free vibration of tuning fork; τ, time, sec; ω, frequency of oscillation of tuning fork, Hz. Subscripts: eff, effective; out, output; ∞, parameters at free oscillation.

REFERENCES

1. G. Binnig, C. F. Quate, and C. Gerber, Atomic force microscope, *Phys. Rev. Lett.*, **56**, 930–933 (1986).
2. C. Bustamante and D. Keller, Scanning force microscopy in biology, *Phys. Today*, **48**, 32–38 (1995).
3. Z. Shao, J. Mou, D. M. Czajkowsky, J. Yang, and J.-Y. Yuan, Biological atomic force microscopy: what is achieved and what is needed, *Adv. Phys.*, **45**, 1–86 (1996).
4. V. V. Tsukruk, Scanning probe microscopy of polymer surfaces, *Rubber Chem. Technol.*, **70**, 430–467 (1997).
5. G. Krausch, M. Hipp, M. Boltau, O. Marti, and J. Mlynek, High resolution imaging of polymer surfaces with chemical sensitivity, *Macromolecules*, **28**, 260 (1995).
6. C. M. Mate, Force microscopy studies of the molecular origins of friction and lubrication, *IBM J. Res. Dev.*, **39**, 617–627 (1995).
7. B. C. Stipe, M. A. Rezaei, and W. Ho, Single molecule vibrational spectroscopy and microscopy, *Science*, **280**, 1732–1735 (1998).
8. C. Durkan and M. E. Welland, Electronic spin detection in molecules using scanning-tunneling microscopy-assisted electron-spin resonance, *Appl. Phys. Lett.*, **80**, 458–460 (2002).
9. D. Lee, A. Wetzel, R. Bennewitz, E. Meyer, M. Despont, P. Vettiger, and C. Gerber, Switchable cantilever for a time-of-flight scanning force microscope, *Appl. Phys. Lett.*, **84**, 1558–1560 (2004).
10. B. Anczykowski, D. Kruger, and H. Fuchs, Cantilever dynamics in quasinoncontact force microscopy: Spectroscopic aspects, *Phys. Rev. B.*, **53**, 15485–15486 (1996).
11. B. Gotsmann, B. Anczykowski, C. Seidel, and H. Fuchs, Determination of tip–sample interaction forces from measured dynamic force spectroscopy curves and computer simulation, *Appl. Surf. Sci.*, **140**, 314–319 (1999).

12. C. L. Pang, T. V. Ashworth, H. Raza, S. A. Haycock, and G. Thornton, A non-contact atomic force microscopy and 'force spectroscopy' study of charging on oxide surfaces, *Nanotechnology*, **15**, 862–866 (2004).
13. P. Guethner, U. Fischer, and K. Dransfeld, Scanning near-field acoustic microscopy, *Appl. Phys. B. Photophys. Laser Chem.*, **B 48**, 89–92 (1989).
14. K. Karrai and R. D. Grober, Piezoelectric tip—sample distance control for near field optical microscopes, *Appl. Phys. Lett.*, **66**, 1842–1844 (1995).
15. F. J. Giessibl, High-speed force sensor for force microscopy and profilometry utilizing a quartz tuning fork, *Appl. Phys. Lett*., **73**, 3956–3958 (1989).
16. J. Rychen, T. Ihn, P. Studerus, A. Herrmann, and K. Ensslin, A low-temperature dynamic mode scanning force microscope operating in high magnetic fields, *Rev. Sci. Instrum*., **70**, 2765–2768 (1999).
17. J. Zang and S. O'Shea, Tuning forks as micromechanical mass sensitive sensors for bio- or liquid detection, *Sensor Actuator*, **94**, 65–72 (2003).
18. W. H. J. Rensen, Imaging soft samples in liquid with tuning fork based shear force microscopy, *Appl. Phys. Lett*., **66**, 1842–1844 (1995).
19. K. Karrai and I. Tiemann, Interfacial shear force microscopy, *Phys. Rev. B*, **62**, 13174–13181 (2000).
20. Vo Thanh Tung, S. A. Chizhik, V. V. Chikunov, Nguyen Tho Vuong, and Tran Xuan Hoai, Influence of additional mass on quartz tuning fork in dynamic operation mode, in: *Proc. 7th Int. BelSPM-7*, Minsk (2006), pp. 236–240.
21. http:// microtm.com/nt206/nt206r.htm.
22. Vo Thanh Tung and S. A. Chizhik, Quartz tuning fork atomic force microscopy using quality-factor control, in: *Proc. Int. Nanomeeting 2007*, Minsk (2007), pp. 535–538.
23. J. M. Fridet and E. Carry, Introduction to the quartz tuning fork, *Am. J. Phys.*, **75**, 415–422 (2007).
24. F. D. Callaghan, X. Yu, and C. J. Mellow, Variable temperature magnetic force microscopy with piezoelectric quartz tuning forks as probes optimized using Q-control, *Appl. Phys. Lett*., **87**, 214106 (2005).